The Atomic Gas Mass of Green Pea Galaxies

N. Kanekar[1] , T. Ghosh[2] , J. Rhoads[3,4] , S. Malhotra[3,4] , S. Harish[4] , J. N. Chengalur[1] , and K. M. Jones[5]

[1] National Centre for Radio Astrophysics, Tata Institute of Fundamental Research, Pune University, Pune 411007, India; nkanekar@ncra.tifr.res.in
[2] Green Bank Observatory, P.O. Box 2, Green Bank, WV 24944, USA
[3] Astrophysics Division, NASA Goddard Space Flight Center, Greenbelt, MD 20771, USA
[4] School of Earth and Space Exploration, Arizona State University, Tempe, AZ 85287, USA
[5] Department of Physics and Astronomy, University of Kansas, 1082 Malott, 1251 Wescoe Hall Drive, Lawrence, KS 66045, USA

Abstract

We have used the Arecibo Telescope and the Green Bank Telescope (GBT) to carry out a deep search for H I 21 cm emission from a large sample of "Green Pea" galaxies, yielding 19 detections, and 21 upper limits on the H I mass. We obtain H I masses of $M_{HI} \approx (4–300) \times 10^8 M_\odot$ for the detections, with a median H I mass of $\approx 2.6 \times 10^9 M_\odot$; for the non-detections, the median 3σ upper limit on the H I mass is $\approx 5.5 \times 10^8 M_\odot$. These are the first estimates of the atomic gas content of Green Pea galaxies. We find that the H I-to-stellar mass ratio in Green Peas is consistent with trends identified in star-forming galaxies in the local universe. However, the median H I depletion timescale in Green Peas is ≈ 0.6 Gyr, an order of magnitude lower than that obtained in local star-forming galaxies. This implies that Green Peas consume their atomic gas on very short timescales. A significant fraction of the Green Peas of our sample lie $\gtrsim 0.6$ dex (2σ) above the local M_{HI}–M_B relation, suggesting recent gas accretion. Further, $\approx 30\%$ of the Green Peas are more than $\pm 2\sigma$ deviant from this relation, suggesting possible bimodality in the Green Pea population. We obtain a low H I 21 cm detection rate in the Green Peas with the highest O32 ≡ [O III] $\lambda5007/$[O II]$\lambda3727$ luminosity ratios, O32 > 10, consistent with the high expected Lyman-continuum leakage from these galaxies.

1. Introduction

The nature of "Green Pea" galaxies, the low-redshift ($z \lesssim 0.3$) extreme emission-line galaxies identified by the Galaxy Zoo project (Cardamone et al. 2009), has been of much interest over the last decade. Their low metallicity and dust content, strong nebular lines, compact or interacting morphology, and intense star formation activity are all reminiscent of high-z Lyα emitters (e.g., Izotov et al. 2011; Yang et al. 2017; Jiang et al. 2019). Indeed, for Green Peas studied at ultraviolet (UV) wavelengths, the Lyα equivalent width distribution is similar to that of Lyα emitters at $z \gtrsim 2.8$ (Yang et al. 2016), while the Lyα and UV continuum sizes are similar to those of Lyα emitters at $z \approx 3 - 6$ (Yang et al. 2017). Green Peas show a high [O III]$\lambda5007/$[O II]$\lambda3727$ luminosity ratio, similar to many high-z star-forming galaxies, indicating optically thin ionized regions (e.g., Jaskot & Oey 2013; Nakajima et al. 2020). Perhaps most interesting, and unlike most galaxies in the low-z universe, Green Peas have been found to commonly show leakage of Lyman-continuum radiation, with escape fractions of $\approx 2.5\%$–73% (Izotov et al. 2016, 2018a, 2018b). Such Lyman-continuum radiation escaping from star-forming galaxies is expected to have been the prime cause of the reionization of the universe, at $z \gtrsim 6$ (e.g., Fan et al. 2006); however, the dependence of the escape fraction on local conditions is still not understood today. Galaxies like the Green Peas that show strong Lyman-continuum leakage are the best low-z analogs of the galaxies that drove cosmological reionization, and offer the exciting possibility of understanding this critical process in the nearby universe.

While detailed optical and UV imaging and spectroscopic studies have characterized the stellar, nebular, and star formation properties of the Green Peas (e.g., Amorín et al. 2010; Izotov et al. 2011, 2018b; Jaskot & Oey 2014; Yang et al. 2016, 2017; Lofthouse et al. 2017; Jiang et al. 2019), little is known about the primary fuel for star formation in these galaxies, the neutral atomic, or molecular gas. As such, the cause of the intense starburst activity in the Green Peas remains unclear. Further, there is a natural tension between requiring cold neutral gas to fuel the starburst activity and having a sufficiently low H I column density to allow the resonantly scattered Lyα and Lyman continuum to escape. This suggests that the H I column density distribution in Green Peas may be highly non-uniform, with H I porosity playing a key role (but see Henry et al. 2015).

At present, only two Green Peas have published searches for H I 21 cm emission, both yielding upper limits on the H I mass of the galaxy (Pardy et al. 2014; McKinney et al. 2019). We report here Arecibo Telescope (hereafter, Arecibo) and Green Bank Telescope (GBT) H I 21 cm spectroscopy of a large sample of Green Peas at $z \approx 0.02 - 0.1$, which allow us to measure the atomic gas mass of these galaxies for the first time.[6]

2. Observations, Data Analysis, and Results

Jiang et al. (2019) have compiled the most comprehensive Green Pea galaxy sample to date, consisting of approximately 1000 galaxies at $0.01 \lesssim z \lesssim 0.41$, identified from the Sloan Digital Sky Survey (SDSS) spectroscopic Data Release 13. We used the correlation between B-band luminosity and H I mass (e.g., Dénes et al. 2014) to pre-select Green Peas from the above sample with H I masses high enough to show detectable H I 21 cm emission with Arecibo and the GBT in reasonable

---

[6] We assume a flat Λ-cold dark matter cosmology, with $\Omega_\Lambda = 0.685$, $\Omega_m = 0.315$, $H_0 = 67.4$ km s^{-1} Mpc^{-1} (Planck Collaboration 2020).

integration time (few hours). Our targets span a wide range of absolute B-band magnitudes ($-20.0 \leqslant M_B \leqslant -16.1$) and gas-phase metallicities ($7.6 \leqslant 12 + [O/H] \leqslant 8.35$). We also carried out two-sample Kolmogorov–Smirnov tests to compare the distributions of metallicity, stellar mass, and absolute B-magnitude in our target sample with those of the parent Green Pea sample of Jiang et al. (2019). We find that the data are consistent with the null hypothesis that the two samples are drawn from the same distribution, in all three parameters.

We used Arecibo and the GBT to carry out a search for H I 21 cm emission from 44 Green Peas, at $z \approx 0.02$–0.1 (proposals GBT/19A-301: PI Malhotra; Arecibo/A3302: PI Rhoads), between 2019 February and August. To use the complementary strengths of Arecibo and the GBT, we observed lower-redshift targets ($z \lesssim 0.05$) with higher expected H I 21 cm line flux densities over the entire northern and equatorial sky using the GBT. With Arecibo, we broadened the selection to include Green Peas with lower expected H I 21 cm line flux densities and higher redshifts ($z \lesssim 0.1$), within the region of sky accessible to the telescope.

The Arecibo observations used the L-wide receiver, the WAPP backend, two orthogonal polarizations, and a 25 MHz band sub-divided into 4096 spectral channels and centered on the redshifted H I 21 cm line frequency. The GBT observations used the L-band receiver with the VEGAS spectrometer as the backend, two polarizations, and a 23.44 MHz bandwidth sub-divided into 8192 channels, and centered on the redshifted H I 21 cm line frequency. Position-switching, with 5 m On and Off scans, was used to calibrate the system bandpass, while the system temperatures were measured using a blinking noise diode at the GBT, and a separate noise diode, switched on and off for 10 s, at Arecibo. Online Doppler tracking was not used. The total time on each source ranged from 0.75 to 4.5 hr, depending on the galaxy redshift, radio frequency interference (RFI) conditions, and observing exigencies.

All data were analyzed in the IDL package, following standard procedures, with the package GBTIDL used for the GBT data. Each On/Off pair was initially calibrated and the final spectrum, for each polarization, shifted into the barycentric frame. Each spectrum was then inspected for the presence of RFI or systematic effects in the spectral baseline; spectra showing non-Gaussian behavior within $\approx \pm 200$ km s^{-1} of the expected redshifted H I 21 cm line frequency were removed from the analysis. For each source, the remaining spectra, from both polarizations, were median-averaged together, with the median used to obtain a more conservative (i.e., less sensitive to outliers) estimate of the average. For four sources, two from each telescope, all spectra were affected by RFI around the expected redshifted line frequency, and the data were essentially unusable.

H I 21 cm emission was detected from 19 Green Peas at $\geqslant 5\sigma$ significance (two of which, in J0844+0226 and J1010+1255, have $\approx 5\sigma$ significance and hence should be viewed as tentative detections); the H I 21 cm spectra of these galaxies are shown in Figure 1. Twenty-one galaxies showed no clear signature of H I 21 cm emission. Table 1 summarizes the results of the Arecibo and GBT observations; we also include the relevant galaxy properties of each Green Pea, derived from the optical imaging and spectroscopy (e.g., Jiang et al. 2019). The upper limits are computed assuming a Gaussian line profile with a full width at half maximum (FWHM) of 50 km s^{-1}, typical of dwarf galaxies (the H I mass limits are mostly $\lesssim 10^9 M_\odot$, i.e., in

the dwarf galaxy range; e.g., Begum et al. 2008). We note that the errors quoted on the H I 21 cm line flux densities and the H I masses are statistical errors, and do not include the uncertainty in the flux scale; we estimate this uncertainty to be typically $\approx 10\%$.

3. Discussion

Our Arecibo and GBT H I 21 cm spectroscopy of Green Pea galaxies has yielded an $\approx 50\%$ detection rate, with 19 detections of H I 21 cm emission at redshifts $z \approx 0.023$–0.091. These are the first measurements of the atomic gas content of Green Pea galaxies. The H I masses of the detected galaxies lie in the range $\approx (4$–$300) \times 10^8 M_\odot$, with a median value of $2.6 \times 10^9 M_\odot$. For the non-detections, the 3σ upper limits on the H I mass lie in the range $(0.6$–$32) \times 10^8 M_\odot$, with a median upper limit of $5.5 \times 10^8 M_\odot$. Note that the large primary beams of Arecibo and the GBT imply that we cannot rule out the possibility that some of the H I 21 cm emission in the detections may arise from companion galaxies.

Figure 2(A) plots the H I-to-stellar mass ratio $f_{HI} \equiv M_{HI}/M_\star$ against the stellar mass $M_\star$ of the 40 Green Peas of our sample. We used the xGASS sample as the comparison sample, as this is a stellar mass-selected ($M_\star \geqslant 10^9 M_\odot$) sample of nearby galaxies, with H I 21 cm emission studies (Catinella et al. 2018). The dark green stars indicate the median value of f_{HI} (treating the 3σ upper limits to f_{HI} as detections) in two stellar mass bins, while the filled blue circles indicate the median values of f_{HI} in galaxies in different stellar mass bins in the GALEX Arecibo SDSS Survey (xGASS) sample (Catinella et al. 2018), with the dashed blue line connecting the xGASS values. It is clear that the median value of f_{HI} for Green Peas in the higher $M_\star$ bin is in excellent agreement with the median value for xGASS galaxies at the same $M_\star$, while the median f_{HI} in the lower $M_\star$ bin appears to lie close to the extrapolated xGASS relation (Catinella et al. 2018). It thus appears that the H I content of Green Pea galaxies, relative to their stellar mass, is in excellent agreement with that of "normal" galaxies in the nearby universe.

The atomic gas depletion timescale $\tau_{dep} \equiv M_{HI}/SFR$ gives the timescale for which a galaxy can continue to form stars without replenishment of its H I reservoir. Lower values of τ_{dep} would imply that a galaxy's star formation activity would be regulated by the availability of H I; for example, Chowdhury et al. (2020) argued that the cause of the decline of the star formation activity in the universe at $z < 1$ is because the H I reservoirs in star-forming galaxies are not sufficient to support their star formation activity for more than ≈ 1–2 Gyr. However, at $z \lesssim 0.35$, the H I depletion timescale has been found to be relatively long in main-sequence galaxies, ≈ 5–10 Gyr (e.g., Saintonge et al. 2017; Bera et al. 2019). Figure 2(B) plots the τ_{dep} values of our Green Pea galaxies against stellar mass; the dashed green line shows the median value of the sample, $\tau_{dep, med} \approx 0.58$ Gyr (conservatively treating the upper limits on M_{HI} as detections). For comparison, the median value of τ_{dep} in the xGASS sample (again treating upper limits to M_{HI} as detections), shown by the dashed blue line in the figure, is ≈ 6 Gyr (Saintonge et al. 2017; Catinella et al. 2018), larger by an order of magnitude. It appears that the starburst activity in the Green Peas will exhaust their atomic fuel on very short timescales, far shorter than in most other galaxies in the nearby universe.
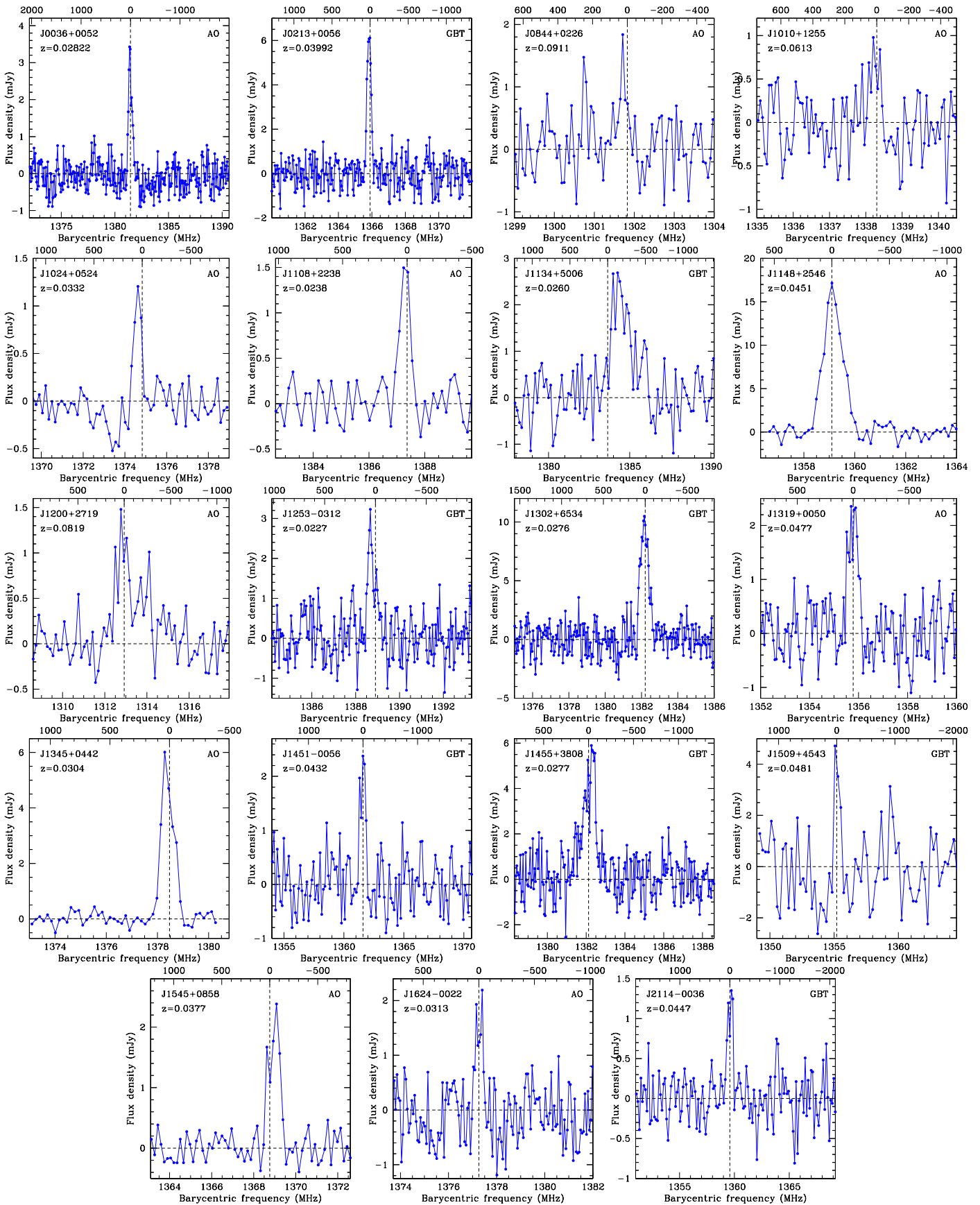
Figure 1. HI 21 cm emission profiles of the 19 Green Peas with HI 21 cm detections, ordered by R.A.. In each panel, the *x*-axis is barycentric frequency, in MHz; the top of the panel shows velocity, in km s^{-1}, relative to the Green Pea redshift (based on the optical spectra). The HI 21 cm spectra have been smoothed to, and resampled at, velocity resolutions of $\approx$10–30 km s^{-1}. Note that the HI 21 cm detections in J0844+0226 and J1010+1255 have $\approx$5σ significance, and so should be treated as tentative detections.

Table 1
Results

Green Pea identifier	z	Tel.	$\nu_{21\,cm}$ (MHz)	$\int S dV$ (Jy km s^{-1})	M_{HI} ($10^8\,M_\odot$)	SFR ($M_\odot$ yr^{-1})	$M_\star$ ($10^8\,M_\odot$)	f_{HI}	τ_{dep} (Gyr)	M_B	O32
J0007+0226	0.0636	1	1335.52	<0.062	<12	0.69	3.0	<4.0	<1.7	−18.64	48.5
J0036+0052	0.0282	1	1381.42	0.585 ± 0.034	22.0 ± 1.3	0.17	1.7	12.8	13.0	−16.41	7.7
J0159+0751	0.0611	1	1338.65	<0.038	<6.9	1.0	0.49	<14.1	<0.67	−17.63	60.5
J0213+0056	0.0399	2	1365.88	0.419 ± 0.022	31.7 ± 1.7	1.4	7.8	4.1	2.3	−17.62	8.8
J0801+3823	0.0376	2	1368.89	<0.051	<3.4	0.57	15.6	<0.22	<0.60	−16.08	3.3
J0808+1728	0.0442	1	1360.28	<0.044	<4.1	0.45	2.9	<1.4	<0.91	−17.84	14.1
J0844+0226	0.0911	1	1301.81	0.065 ± 0.013	26.1 ± 5.4	14.0	125.9	0.21	0.19	−19.65	4.1
J0852+1216	0.0759	1	1320.19	<0.050	<14	13.4	73.0	<0.19	<0.10	−18.32	4.0
J0942+4110	0.0460	2	1357.97	<0.125	<13	2.6	6.7	<1.9	<0.49	−18.92	11.5
J1010+1255	0.0613	1	1338.31	0.053 ± 0.011	9.6 ± 2.0	5.3	6.7	1.4	0.18	−20.02	4.2
J1015+3054	0.0918	1	1301.04	<0.037	<15	6.1	19.2	<0.78	<0.25	−19.88	2.3
J1024+0524	0.0332	1	1374.76	0.074 ± 0.014	3.85 ± 0.73	1.6	0.95	4.0	0.25	−18.91	5.6
J1108+2238	0.0238	1	1387.37	0.155 ± 0.016	4.14 ± 0.43	0.58	5.6	0.74	0.71	−16.89	2.8
J1134+5006	0.0260	2	1384.44	0.799 ± 0.065	25.4 ± 2.1	2.2	0.98	25.8	1.1	−18.24	2.5
J1148+2546	0.0451	1	1359.07	3.182 ± 0.078	309.0 ± 7.6	5.2	5.7	54.7	6.0	−19.52	5.4
J1200+2719	0.0819	1	1312.91	0.310 ± 0.028	100.6 ± 9.0	3.8	20.0	4.6	2.5	−18.83	12.9
J1224+0105	0.0398	2	1365.99	<0.063	<4.8	0.85	15.0	<0.32	<0.56	−17.12	3.4
J1224+3724	0.0404	2	1365.25	<0.077	<5.9	0.96	4.0	<1.5	<0.62	−17.87	8.6
J1226+0415	0.0942	1	1298.10	<0.073	<32	5.1	29.0	<1.1	<0.62	−19.99	11.2
J1253-0312	0.0227	2	1388.89	0.235 ± 0.021	56.9 ± 5.1	89.2	1.3	41.8	0.062	−19.58	4.6
J1302+6534	0.0276	2	1382.20	1.179 ± 0.052	42.6 ± 1.9	0.69	11.1	3.8	6.2	−17.51	3.9
J1319+0050	0.0477	1	1355.78	0.234 ± 0.025	21.7 ± 2.3	1.4	9.8	2.2	1.6	−17.99	2.7
J1329+1700	0.0942	1	1298.16	<0.086	<37	9.9	49.1	<0.75	<0.37	−18.65	4.0
J1345+0442	0.0304	1	1378.47	0.650 ± 0.026	28.5 ± 1.1	1.1	7.2	4.0	2.6	−17.80	3.0
J1359+5726	0.0338	2	1373.93	<0.095	<5.1	2.1	13.3	<0.38	<0.24	−17.28	3.6
J1411+0556	0.0493	2	1353.62	<0.047	<5.5	1.4	1.4	<3.9	<0.40	−19.88	19.6
J1423+2257	0.0328	1	1375.24	<0.025	<1.3	0.98	1.5	<0.89	<0.13	−17.16	8.5
J1432+5152	0.0256	2	1384.94	<0.079	<2.4	0.58	9.5	<0.26	<0.43	−17.38	3.3
J1448-0110	0.0274	2	1382.50	<0.054	<1.9	2.8	0.84	<2.3	<0.068	−18.62	10.2
J1451-0056	0.0432	2	1361.59	0.288 ± 0.029	25.6 ± 2.6	0.63	11.1	2.3	4.0	−18.38	3.5
J1455+3808	0.0277	2	1382.13	0.855 ± 0.047	31.0 ± 1.7	0.96	2.2	14.4	3.2	−17.56	7.5
J1509+3731	0.0326	2	1375.58	<0.088	<4.4	1.77	0.86	<5.2	<0.25	−18.41	19.2
J1509+4543	0.0481	2	1355.18	0.543 ± 0.081	60.0 ± 8.9	3.3	37.8	1.6	1.8	−18.66	3.1
J1518+1955	0.0751	1	1321.19	<0.041	<11	4.93	31.7	<0.35	<0.22	−19.47	3.3
J1545+0858	0.0377	1	1368.76	0.302 ± 0.019	17.8 ± 1.1	4.4	10.1	1.8	0.40	−18.91	9.7
J1547+2203	0.0314	1	1377.15	<0.053	<2.5	0.68	8.5	<0.29	<0.37	−17.31	5.9
J1608+3528	0.0327	1	1375.38	<0.12	<0.61	0.46	0.29	<2.1	<0.13	−17.01	51.1
J1624-0022	0.0313	1	1377.27	0.134 ± 0.021	62.2 ± 9.8	4.0	13.0	4.8	1.6	−17.22	5.0
J2114-0036	0.0447	2	1359.59	0.173 ± 0.020	16.5 ± 1.9	0.79	2.2	7.6	2.1	−19.67	9.3
J2302+0049	0.0331	1	1374.91	<0.050	<2.6	0.49	1.0	<2.5	<0.53	−16.91	11.6

Note. The columns are (1) the Green Pea galaxy identifier, (2) the galaxy redshift, (3) the telescope used for the observations (Arecibo ≡ 1, GBT ≡ 2, (4) the expected redshifted HI 21 cm line frequency, (5) the velocity-integrated HI 21 cm line flux density (and error), or 3σ upper limits to this quantity, in Jy km s^{-1}, (6) the inferred HI mass (and error), in units of $10^8\,M_\odot$, (7) the star formation rate (SFR), in $M_\odot$ yr^{-1} (Jiang et al. 2019), (8) the stellar mass, in units of $10^8\,M_\odot$ (Jiang et al. 2019), (9) the HI-to-stellar mass ratio, $f_{HI} \equiv M_{HI}/M_\star$, (10) the HI depletion time, in Gyr, (11) the absolute blue magnitude, M_B, and (12) the ratio of the luminosities in the [O III]λ5007 and [O II]λ3727 lines, O32 ≡ [O III]λ 5007/[O II]λ3727.

The depletion time of star-forming material could be longer than the HI depletion timescale when the H_2 depletion timescale is taken into account. However, in star-forming galaxies at all redshifts, the H_2 depletion timescale is typically $\lesssim 1$ Gyr (e.g., Saintonge et al. 2017; Tacconi et al. 2020), far shorter than the HI depletion timescale. As such, star formation in such galaxies is not limited by the depletion of HI, as there is a long timescale on which the HI can be replenished from the circumgalactic medium. However, the very short HI depletion time in Green Peas implies that HI depletion could itself act as a bottleneck for star formation (as has been seen in main-sequence galaxies at $z \approx 1$; Chowdhury et al. 2020).

Figure 3(A) plots the HI mass of the Green Peas against their absolute B-magnitude M_B; the dashed line indicates the M_{HI}–M_B relation of galaxies in the local universe, with the dotted lines indicating the ±0.6 dex ($\approx 2\sigma$) spread around the local relation (e.g., Dénes et al. 2014). While the majority of the Green Peas are seen to lie within the spread of the local M_{HI}–M_B relation, it is interesting that nine of the 40 galaxies of our sample (i.e., ≈ 22%) lie $\gtrsim 0.6$ dex above it. This suggests that a significant fraction of Green Peas are gas-rich for their optical luminosity, possibly due to recent gas accretion from the circumgalactic medium or via a minor merger, or due to a gas-rich companion galaxy within the relatively large GBT or Arecibo beam.

Conversely, five of the non-detections and two of the detections of HI 21 cm emission lie $\gtrsim 0.6$ dex *below* the local M_{HI}–M_B relation. Further, most of the detections of HI 21 cm emission lie above the local relation, while most of the non-detections lie below it. This may suggest bimodality in the HI
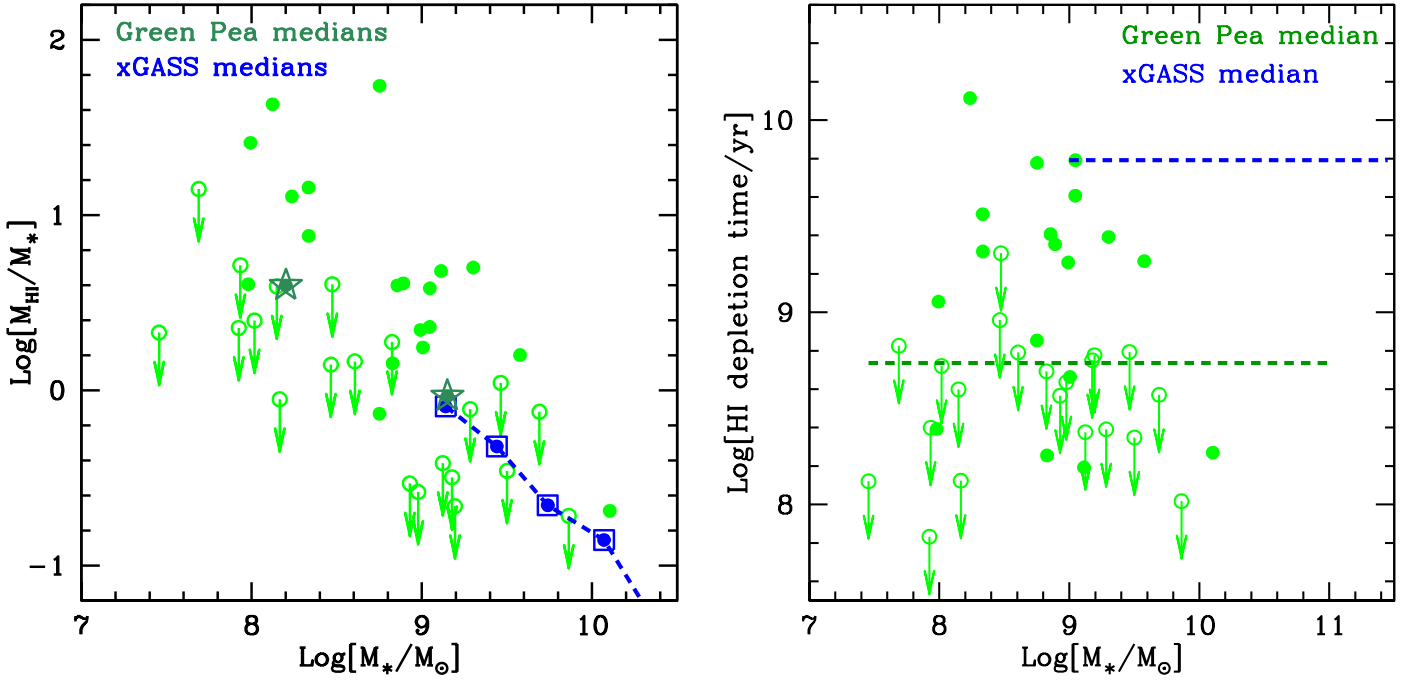
Figure 2. [A] HI-to-stellar mass ratio $f_{HI} \equiv M_{HI}/M_\star$ plotted against the stellar mass $M_\star$, for the 40 Green Peas. Detections of HI 21 cm emission are shown as filled (green) circles, and non-detections as open circles with downward-pointing arrows. The two dark green stars show the median values of f_{HI} in two stellar mass bins. The filled blue circles indicate the median values of f_{HI} in the xGASS sample (Catinella et al. 2018). [B] HI depletion time, τ_{dep}, plotted against the stellar mass $M_\star$ for the Green Pea galaxies. The dashed lines indicate the median HI depletion timescales for the Green Peas (green) and galaxies from the xGASS sample (blue; Saintonge et al. 2017). The median HI depletion timescale of the Green Peas is seen to be an order of magnitude lower than that of the xGASS galaxies.
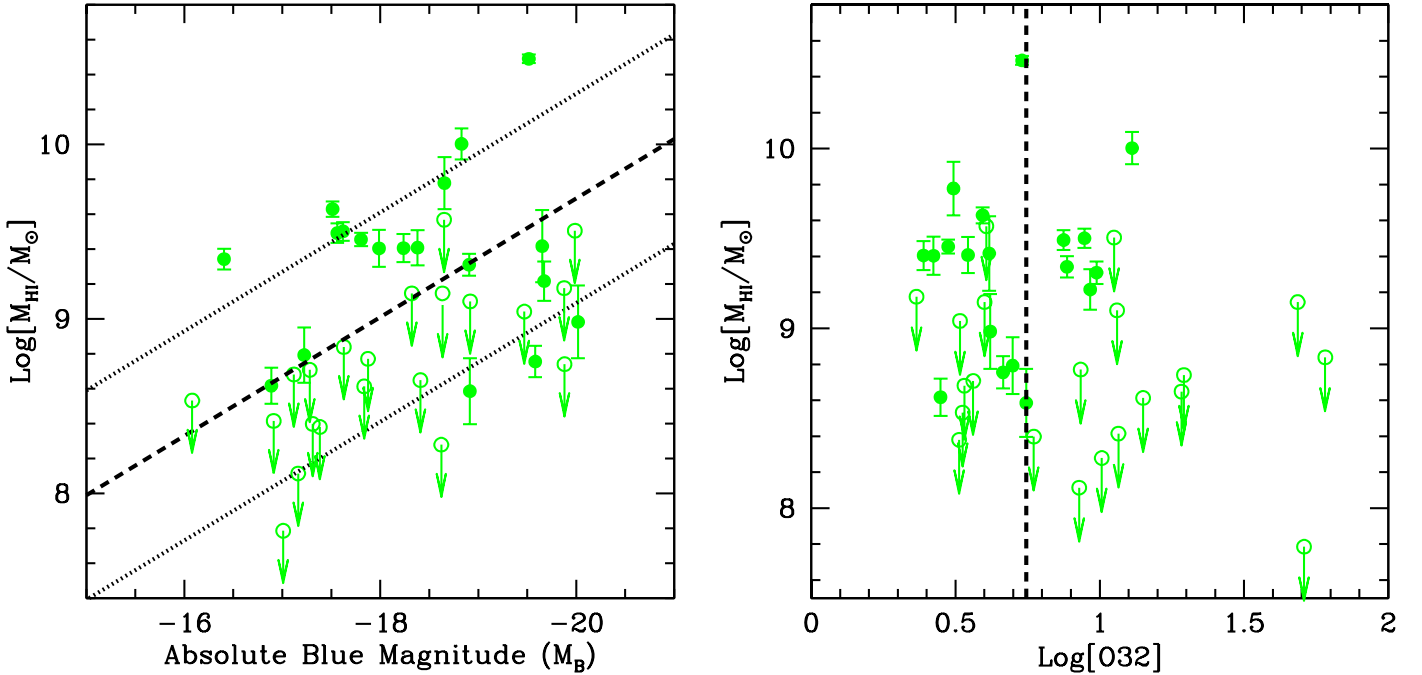
Figure 3. HI mass of the Green Peas plotted against [A] their absolute B-magnitude, M_B, and [B] their O32 value. In [A], the dashed line indicates the M_{HI}–M_B relation in the local universe, while the dotted lines indicate the ± 0.6 dex (i.e., $\pm 2\sigma$) spread around the relation (Dénes et al. 2014). A number of the Green Peas are seen to have HI masses $\gtrsim +0.6$ dex above the local relation, while a few have HI masses $\gtrsim 0.6$ dex below the relation. In [B], the dashed vertical line indicates the median O32 value, ≈ 5.5.

properties of Green Pea galaxies, with one group having exhausted its neutral gas in the starburst (which may have been itself triggered by a recent gas acquisition via infall or a merger), and the other having only consumed a fraction of its

neutral gas in the starburst. We note that a caveat to the above result is that the M_{HI}–M_B relation of Dénes et al. (2014) is based on an HI-selected galaxy sample from the all-sky HI Parkes All Sky Survey (HIPASS; Zwaan et al. 2005), and thus

may be biased toward HI-rich galaxies. As such, objects lying below the M_{HI}–M_B relation of Dénes et al. (2014) may not necessarily be HI-poor galaxies.

Despite the above caveat, it is tempting to identify the first group of galaxies above with the objects that are likely to show leakage of Lyα and Lyman-continuum radiation (i.e., to show Lyα *emission*). Eight of the Green Peas of our sample have Lyα spectroscopy, with seven detections of Lyα emission and one (J1448-0110) showing net Lyα absorption (McKinney et al. 2019). Interestingly, five of the detections of Lyα emission are not detected in HI 21 cm emission, as expected from the above argument. However, two of the Lyα-emitting galaxies, J0213+0056 and J1200+2719, do show detections of HI 21 cm emission, and with relatively high HI masses, $\approx 3.2 \times 10^9 M_\odot$ (J0213+0056) and $\approx 1 \times 10^{10} M_\odot$ (J1200 +2719). Further, both these galaxies are "gas-rich" systems in Figure 3(A). HI 21 cm mapping studies are needed to test whether the Green Pea galaxy itself is HI-rich, or if it might have a gas-rich companion. Such HI 21 cm mapping studies are also critical to directly determine the HI column density distribution within the Green Peas, to test for the presence of HI holes through which the Lyα and Lyman-continuum photons might escape. At any event, at the present time, no clear trend is apparent between the gas richness of the above eight Green Peas and their Lyα escape fraction, with high Lyα escape fractions obtained at both high and low HI masses (and gas richness) in the relatively small current sample (McKinney et al. 2019). Deeper HI 21 cm emission studies would be needed to test the possibility of bimodality in the gas content of Green Pea galaxies.

We also examined the dependence of the HI mass, HI-to-stellar mass ratio, and HI depletion time, on the metallicity (12+[O/H]) of the Green Peas of our sample, finding no evidence of a dependence of any of these properties on the metallicity.

Jaskot & Oey (2013) argued that the high luminosity ratio O32 $\equiv$ [O III]λ5007/[O IIλ3727 observed in a number of Green Pea galaxies at $z \approx 0.1$–0.3 makes them excellent candidates for the escape of ionizing Lyman-continuum radiation. A high Lyman-continuum leakage was indeed later found in galaxies with high O32 values, both at high redshifts (e.g., Nakajima & Ouchi 2014; Nakajima et al. 2016; Fletcher et al. 2019) and low redshifts (including Green Pea galaxies; e.g., Izotov et al. 2016, 2018a, 2018b, 2020), for typical O32 values $\gtrsim 10$. One would expect easier leakage of Lyman-continuum photons from galaxies with a lower average HI column density, and also with a lower HI mass. We hence examined the HI properties in our Green Peas as a function of their O32 value; Figure 3[B] shows the measured HI mass for the 40 Green Peas plotted against the O32 values; the median O32 value is ≈ 5.5, indicated by the dashed vertical line. Among the 20 Green Peas with O32 values below the median, there are 12 detections of HI 21 cm emission, with an average HI mass of $5.6 \times 10^9 M_\odot$, while for Green Peas with O32 values above the median there are seven detections and an average HI mass of $3.2 \times 10^9 M_\odot$. Further, there is only a single detection of HI 21 cm emission in the 11 Green Peas with O32 $\geqslant 10$ (i.e., a detection fraction of $0.091^{+0.21}_{-0.02}$), and 18 detections in the 29 Green Peas with O32 < 10 (i.e., a detection fraction of $0.62^{+0.18}_{-0.14}$). Thus, although the numbers are still small, both the detection rate and the average HI mass appear to be significantly lower in galaxies with O32 $\gtrsim 10$, consistent with the expected high Lyman-continuum leakage.

Tilvi et al. (2009) modeled star formation in Lyα emitters by assuming that the accretion of gas rapidly results in star formation, to obtain a star formation efficiency ($f_\star$) of $\approx 2.5\%$. This is similar to the estimate of $f_\star \approx 4 - 8\%$ obtained by Baldry et al. (2008), by comparing the cosmic stellar mass density to the cosmic baryon density (see also Fukugita et al. 1998). Assuming $f_\star \approx 2.5\%$ yields a median star formation timescale of $\tau_{SF} \approx f_\star \times (M_{HI}/SFR)_{med} \equiv f_\star \times \tau_{dep,med} \approx 15$ Myr. Interestingly, this is similar to the age of the young stellar population that dominates the starlight of the Green Peas of our sample ($\approx$3–8 Myr, with a median age of $\approx$4 Myr; Jiang et al. 2019). We note, however, that the above $f_\star$ estimates (Baldry et al. 2008; Tilvi et al. 2009) are for all baryonic material, including the ionized gas. The agreement between the star formation timescale and the age of the young stellar population in Green Peas might then suggest that the timescale of conversion from ionized gas to neutral gas is short in these galaxies.

4. Summary

We report an Arecibo and GBT search for HI 21 cm emission from a large sample of Green Pea galaxies at $z \approx 0.02 - 0.1$, obtaining 19 detections of HI 21 cm emission and 21 upper limits to the HI mass, and yielding the first estimates of the gas content of these starbursting systems. The HI properties of the majority of the Green Peas appear similar to those of galaxies in the local universe, in terms of the HI-to-stellar mass ratio and the M_{HI}–M_B relations. However, a significant fraction of the Green Peas ($\approx$22%) have an HI mass that is $\gtrsim +0.6$ dex (i.e., $\gtrsim 2\sigma$) above the local M_{HI}–M_B relation, indicating either recent gas accretion or a gas-rich companion galaxy. A similar fraction lie $\gtrsim 0.6$ dex below the local relation, suggesting possible bimodality in the gas properties of Green Peas. This large fraction of outliers ($\approx$30%) from the $M_{HI} - M_B$ relation and the young ages of the stellar populations are indicative of a possible "boom and bust" nature of star formation in Green Peas. Further, the HI depletion times in Green Peas are an order of magnitude lower than values in local galaxies, indicating that the starburst activity will consume their HI on timescales less than a Gyr. The detection rate of HI 21 cm emission appears low in galaxies with the highest O32 values, O32 $\geqslant 10$, consistent with the high Lyman-continuum leakage expected from these galaxies.

---

[7] *"Límites", Jorge Luís Borges.*

ORCID iDs

N. Kanekar ● https://orcid.org/0000-0002-9757-7206
T. Ghosh ● https://orcid.org/0000-0003-4454-2875
J. Rhoads ● https://orcid.org/0000-0002-1501-454X
S. Malhotra ● https://orcid.org/0000-0002-9226-5350
S. Harish ● https://orcid.org/0000-0003-0129-2079
J. N. Chengalur ● https://orcid.org/0000-0002-0269-1154

References

Amorín, R. O., Pérez-Montero, E., & Vílchez, J. M. 2010, ApJL, 715, L128
Baldry, I. K., Glazebrook, K., & Driver, S. P. 2008, MNRAS, 388, 945
Begum, A., Chengalur, J. N., Karachentsev, I. D., Sharina, M. E., & Kaisin, S. S. 2008, MNRAS, 386, 1667
Bera, A., Kanekar, N., Chengalur, J. N., & Bagla, J. S. 2019, ApJL, 882, L7
Cardamone, C., Schawinski, K., Sarzi, M., et al. 2009, MNRAS, 399, 1191
Catinella, B., Saintonge, A., Janowiecki, S., et al. 2018, MNRAS, 476, 875
Chowdhury, A., Kanekar, N., Chengalur, J. N., Sethi, S., & Dwarakanath, K. S. 2020, Natur, 586, 369
Dénes, H., Kilborn, V. A., & Koribalski, B. S. 2014, MNRAS, 444, 667
Fan, X., Carilli, C. L., & Keating, B. 2006, ARA&A, 44, 415
Fletcher, T. J., Tang, M., Robertson, B. E., et al. 2019, ApJ, 878, 87
Fukugita, M., Hogan, C. J., & Peebles, P. 1998, ApJ, 503, 518
Henry, A., Scarlata, C., Martin, C. L., & Erb, D. 2015, ApJ, 809, 19
Izotov, Y. I., Guseva, N. G., & Thuan, T. X. 2011, ApJ, 728, 161
Izotov, Y. I., Schaerer, D., Thuan, T. X., et al. 2016, MNRAS, 461, 3683
Izotov, Y. I., Schaerer, D., Worseck, G., et al. 2018a, MNRAS, 474, 4514
Izotov, Y. I., Schaerer, D., Worseck, G., et al. 2020, MNRAS, 491, 468
Izotov, Y. I., Worseck, G., Schaerer, D., et al. 2018b, MNRAS, 478, 4851
Jaskot, A. E., & Oey, M. S. 2013, ApJ, 766, 91
Jaskot, A. E., & Oey, M. S. 2014, ApJL, 791, L19
Jiang, T., Malhotra, S., Yang, H., & Rhoads, J. E. 2019, ApJ, 872, 146
Lofthouse, E. K., Houghton, R. C. W., & Kaviraj, S. 2017, MNRAS, 471, 2311
McKinney, J. H., Jaskot, A. E., Oey, M. S., et al. 2019, ApJ, 874, 52
Nakajima, K., Ellis, R. S., Iwata, I., et al. 2016, ApJL, 831, L9
Nakajima, K., Ellis, R. S., Robertson, B. E., Tang, M., & Stark, D. P. 2020, ApJ, 889, 161
Nakajima, K., & Ouchi, M. 2014, MNRAS, 442, 900
Pardy, S. A., Cannon, J. M., Östlin, G., et al. 2014, ApJ, 794, 101
Planck Collaboration, Aghanim, N., Akrami, Y., et al. 2020, A&A, 641, A6
Saintonge, A., Catinella, B., Janowiecki, S., et al. 2018, MNRAS, 476, 875
Saintonge, A., Catinella, B., Tacconi, L. J., et al. 2017, ApJS, 233, 22
Tacconi, L. J., Genzel, R., & Sternberg, A. 2020, ARA&A, 58, 157
Tilvi, V., Malhotra, S., Rhoads, J. E., et al. 2009, ApJ, 704, 724
Yang, H., Malhotra, S., Gronke, M., et al. 2016, ApJ, 820, 130
Yang, H., Malhotra, S., Rhoads, J. E., et al. 2017, ApJ, 838, 4
Zwaan, M. A., Meyer, M. J., Staveley-Smith, L., & Webster, R. L. 2005, MNRAS, 359, L30